

Supplemental Material: The Thermodynamic Origins of Chiral Twist in Monolayer Assemblies of Rod-like Colloids

Yawei Liu,^{1,2,*} Jared A. Wood,^{1,3} Achille Giacometti,^{4,5} and Asaph Widmer-Cooper^{1,3,†}

¹*ARC Centre of Excellence in Exciton Science, School of Chemistry,
University of Sydney, Sydney, New South Wales 2006, Australia*

²*Beijing Key Laboratory of Ionic Liquids Clean Process,
CAS Key Laboratory of Green Process and Engineering,*

*State Key Laboratory of Multiphase Complex Systems, Institute of Process Engineering,
Chinese Academy of Sciences, Beijing, 100190, China*

³*The University of Sydney Nano Institute, University of Sydney, Sydney, New South Wales 2006, Australia*

⁴*Dipartimento di Scienze Molecolari e Nanosistemi, Università Ca' Foscari di Venezia Campus Scientifico,
Edificio Alfa, via Torino 155, 30170 Venezia Mestre, Italy*

⁵*European Centre for Living Technology (ECLT) Ca' Bottacin, 3911 Dorsoduro Calle Crosera, 30123 Venice, Italy*

S1. Effect of the number of spheres in one rod

For all results reported in the main text, the contour length $L = 10$ and there are 21 spheres evenly distributed in each rod (i.e. the distance between consecutive spheres is $0.5D$). We confirmed that this model is smooth enough to remove side effects associated with grooves between overlapping spheres. Fig. S1 shows that using more spheres in each rod yields similar results.

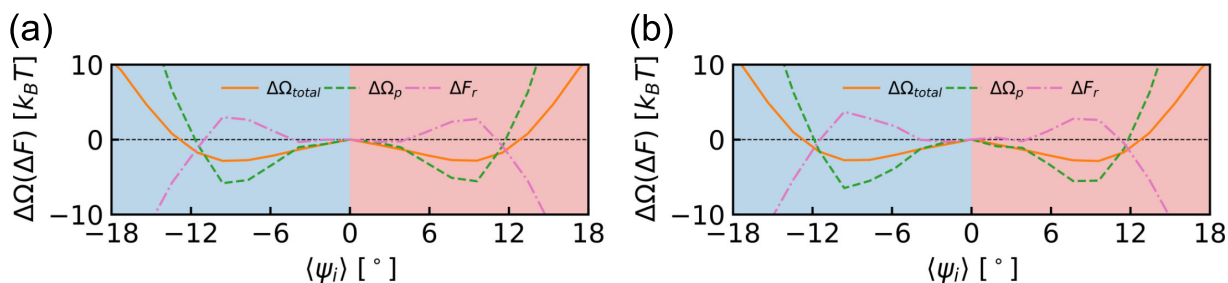


FIG. S1. The total free energy ($\Delta\Omega_{total}$) and its decomposition (ΔF_r and $\Delta\Omega_p$) as a function of the degree of the twist ($\langle\psi_i\rangle$) for a monolayer formed by $N_r = 37$ straight rods with (a) 21 and (b) 41 spheres in each rod.

S2. Effect of the bin size to determine the excluded volume

To compute the excluded volumes during the umbrella sampling simulations, the whole system was divided into many small cubic bins with an edge length of $l = 0.5D$. We confirmed that using a smaller value of l (e.g., $l = 0.25D$, Fig. S2) gave similar results.

S3. Free energy changes for monolayers composed of different numbers of rods

We performed a series of umbrella sampling simulations to calculate the change in free energy as a function of the twist for monolayers formed by $N_r = 2 - 61$ rods with $L = 10$, $r = 0.1$ and varying p . The obtained results shown in Fig. S3 suggest that when $N_r \geq 19$, the free energy minima in these curves are consistent with the phase behavior reported in Fig. 2 (a) in the main text, as discussed in the main text.

* Corresponding author: ywliu@ipe.ac.cn

† Corresponding author: asaph.widmer-cooper@sydney.edu.au

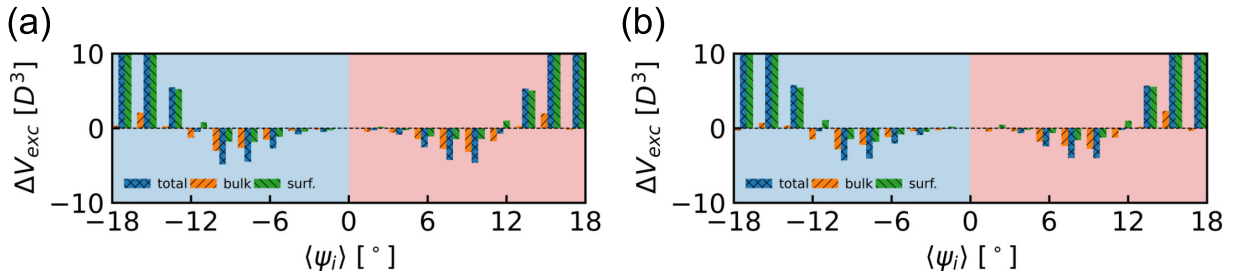


FIG. S2. The change in the total excluded volume (ΔV_{exc}) as a function of $\langle \psi_i \rangle$ and its decomposition into bulk and surface contributions (ΔV_{exc}^{bulk} and ΔV_{exc}^{surf}) for monolayers of 37 straight rods. In the calculations, the edge length of the cubic volumetric bins was $0.5D$ in (a) and $0.25D$ in (b).

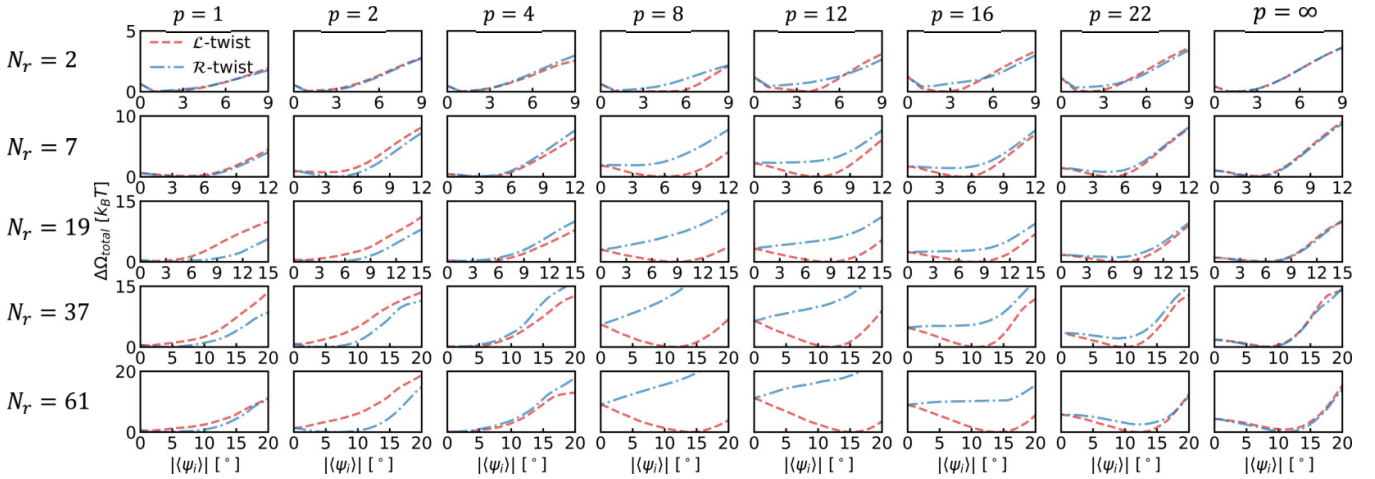


FIG. S3. The total free energy change ($\Delta \Omega_{total}$) as a function of the twist ($\langle \psi_i \rangle$) for monolayers formed by $N_r = 2 - 61$ rods with $L = 10$, $r = 0.1$ and varying p .

We also examined the free energy of twisting for larger monolayers. For computational efficiency, this work was performed using Monte Carlo (MC) simulations of the standard hard AO interaction model[S1]. The same rod length and polymer size was used as in the rest of the paper, with natural twisting observed at a polymer packing fraction of 0.467 and pressure of 1.2. Staged umbrella sampling[S2] with the same bias as in the main text was then used to determine the change in Gibbs free energy as a function of the average tilt angle for several different monolayer sizes, with the free energy profiles assembled using the MBAR technique[S3]. The results are shown in Fig. S4 and are consistent with the results presented in Fig. S3 (at bottom right) for $N_r = 61$.

There are two notable changes as the size of the monolayer increases. First, the magnitude of the preferred average twist increases with the size of the cluster, despite the fraction of rods at the edge of the cluster shrinking with increasing cluster size. This indicates that the local twist at the edge has yet to reach its limiting value of 90° . Once that occurs, we expect the average twist to reach a maximum value and then to gradually decrease. Second, the depth of the free energy minimum, and consequently the free energy barrier to reversing twist direction, increases with size. This increase is roughly linear with the number of rods and monolayer area.

S4. Brief review of the continuum theory for colloidal membranes

In the continuum theory [S4], the colloidal membrane is treated as a continuum medium composed of rods at constant density, and the membrane has a fixed number of rods and a constant volume. In the membrane, a rod at \mathbf{x} (i.e. a given position in the membrane plane) is tilted by $\theta(\mathbf{x})$ with respect to the normal director. The membrane half-thickness can be written as $h(\mathbf{x}) = t \cos \theta(\mathbf{x}) + b(\mathbf{x})$ where t is the half-length of the rod and $b(\mathbf{x})$ is the height fluctuation amplitude of the rod. Assuming

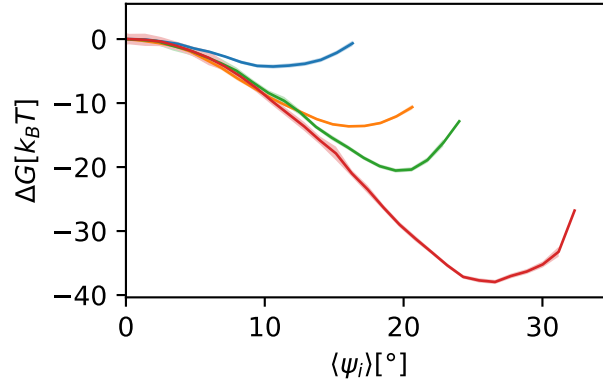


FIG. S4. The change in Gibbs free energy (ΔG) as a function of the twist ($\langle\psi_i\rangle$) for monolayers formed by $N_r = 61$ straight rods (Blue), $N_r = 120$ (Orange), $N_r = 240$ (Green), and $N_r = 480$ (Red). Shaded areas indicate one standard error of the mean.

a circularly-symmetric membrane of radius R and using cylindrical coordinates, one can have $h(r)$, $b(r)$, and $\theta(r)$ that only depend on the radial coordinate.

The free energy associated with the twist distortion of the rods is described by the Frank elastic free energy. Using the one-constant approximation, the free energy is given by

$$F_{\text{Frank}} = 2\pi K \int_0^R dr h \left[r(\partial_r \theta)^2 + \sin 2\theta \partial_r \theta + \frac{\sin^2 \theta}{r} - 2qr \partial_r \theta - q \sin 2\theta \right], \quad (\text{S1})$$

where K is the Frank elastic constant and q is the preferred twist wavenumber associated with the intrinsic chirality of the constituent rods.

The free energy of the polymers is related to the volume excluded to them by the rods. For polymers small compared to the dimensions of the membrane, this excluded volume is approximately $V_0 + aA$, where V_0 is the volume of the membrane, A is the surface area of the membrane, and a is the polymer characteristic radius. V_0 is assumed to be constant, so the corresponding free energy is similar to an effective surface tension, which is expressed as

$$F_{\text{polymer}} = 4\pi n a k_B T \left[\int_0^R dr r \sqrt{1 + (\partial_r h)^2} + R h(R) \right], \quad (\text{S2})$$

where n is the polymer concentration.

If the rod fluctuations perpendicularly to the membrane plane are ignored, then $h \approx t \cos \theta$, and the profile of the membrane is can be obtained by minimizing the total free energy over $h(r)$ using a volume-conserving Lagrange multiplier λ , i.e.,

$$F = F_{\text{Frank}} + F_{\text{polymer}} + \lambda \left[V_0 - 4\pi \int_0^R dr r h \right], \quad (\text{S3})$$

In this continuum theory, the key points for the twist are:

- The preferred handedness in membranes composed of chiral rods is entirely determined by the non-zero q through the free energy of the rods. For example, when $q > 0$, twisted membranes with $\partial_r \theta > 0$ have lower energy than those with $\partial_r \theta < 0$.
- The polymer entropy drives the twist via minimizing the excluded volume, but it is invariant under the chirality inversion $\theta \rightarrow -\theta$, and thus does not contribute to the preferred handedness regardless of the intrinsic chirality of the rods (i.e. q).
- The excluded volume only depends on the surface area of the membrane since the volume of the membrane is assumed to be constant.

The rod fluctuations perpendicular to the membrane plane have complicated, non-linear effects on the free energy, and so are very difficult to accurately account for in the theory. The continuum theory in Ref. [S4] only considered fluctuations of single rods and thus ignored their interactions and correlated motion. The corresponding free energy was calculated in the small rod angle and small fluctuation amplitude limit, and the rods were assumed to be packed hexagonally and to maintain a constant perpendicular distance ξ between nearest-neighbors. Under these assumptions, the rod fluctuation free energy is given by

$$F_{\text{fluctuation}} = \frac{8\pi^2 n a k_B T}{\sqrt{3}\xi^2} \int_0^R dr r \cos \theta \left[h - t \cos \theta - (2\pi n a)^{-1/2} \right]. \quad (\text{S4})$$

S5. Density profiles and volume changes of assembled monolayers

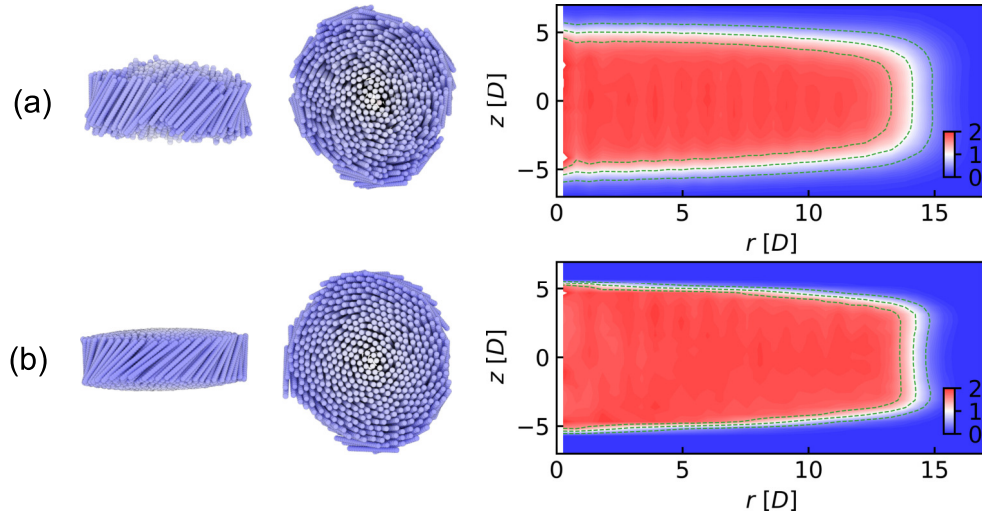


FIG. S5. The snapshots and the density profile for (a) a free monolayer suspended in nonadsorbing polymers (b) a confined monolayer with centers of all rods fixed at the 2D midplane. The dashed lines are density contours at $\rho = 0.5, 1.0, \text{ and } 1.5 D^{-3}$. The slightly concave contour lines in (b) are the results of the hyperboloid-like shape. All monolayers are made up of (achiral) straight rods.

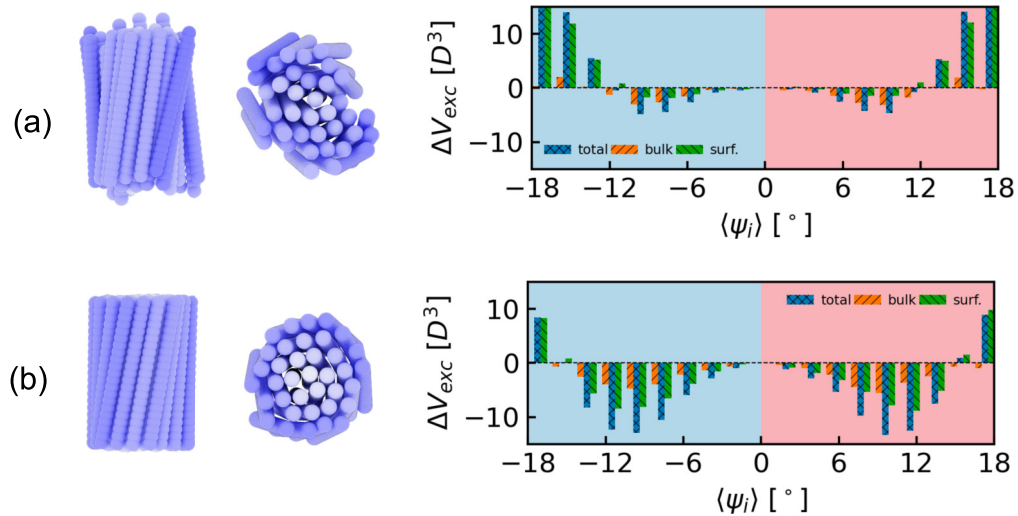


FIG. S6. The changes of excluded volume for the two monolayers made up of 37 straight rods. (a) A free monolayer suspended in nonadsorbing polymers. (b) A confined monolayer with centers of all rods fixed at the 2D midplane.

S6. Monolayers held together by explicit attraction

We observed similar twisting behavior in the absence of polymer depletion when the rods interacted with each other via an explicit attractive potential. In this model, the rods consisted of 40 spheres over a length $L = 10$ with the spheres in different rods interacting with each other via a square well potential of width $w = 1$ and depth $1/20^2 = 0.0025\epsilon_0$, and the temperature scaled to $T = k_B T / \epsilon_0$. There was no polymer in the model, with rod-attraction coming only from the square well interactions. All

work was performed using monolayers of 61 rods. Using the same MC simulation and umbrella sampling approach described in section S3, this time in the NVT ensemble, we calculated the Helmholtz free energy change (ΔF) along with the change in the mean potential energy (ΔU) as a function of the average twist. Using this, we also determined the entropy contribution to ΔF using $-T\Delta S = \Delta F - \Delta U$.

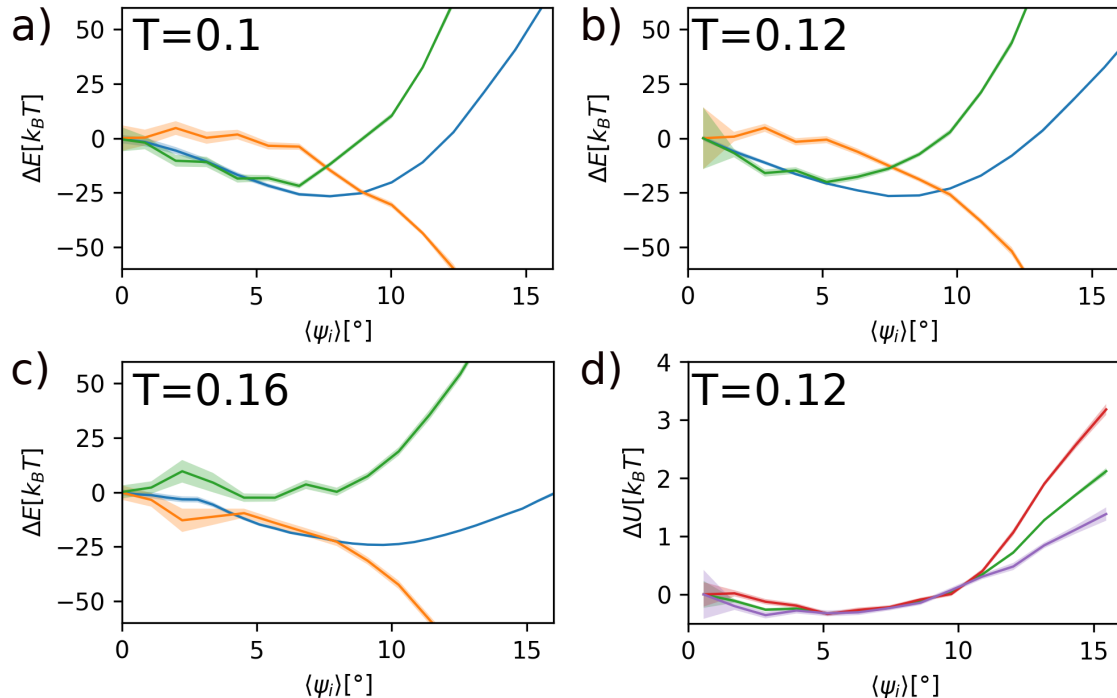


FIG. S7. The change in free energy ΔF (Blue) and its decomposition into $-T\Delta S$ (Orange) and ΔU (Green) as a function of twist for monolayers formed by $N_r = 61$ square-well rods at temperatures of a) $T = 0.1$, b) $T = 0.12$, and c) $T = 0.16$. d) Shows ΔU normalized by the number of rods for all rods in the monolayer (Green), for rods located at the edge of the monolayer (Red), and for rods located in the interior (Purple). Shaded areas indicate one standard error of the mean.

The energy changes obtained as a function of the twist angle at three different temperatures are shown in Fig. S7 (a-c). At the lower temperatures ($T = 0.1$ and $T = 0.12$), the initial twisting is driven entirely by the potential energy of the rods, with the rod entropy only becoming a significant driver at higher angles. This is similar to what we observed for straight rods when the twisting was driven by depletion-attraction [Fig.3a (i) in the main text]. In that case, the rod free energy ΔF_r , which is analogous to $-T\Delta S$ in this model, opposes twisting at small angles and only drives it at larger angles. Similarly, the force holding the monolayer together in both models ($\Delta\Omega_p$ and ΔU) favors small twists but opposes larger ones.

Breaking down the potential energy into contributions from (i) rods in the interior of the monolayer and (ii) those at the edge, provides insight into whether the initial twisting is driven by minimization of the surface energy of the monolayer. This breakdown is shown for $T = 0.12$ in Fig. S7 (d). Surprisingly, we find very little difference in the potential energy change per rod between the different subgroups until past the optimum twist angle, counter-intuitively indicating that the edge of the monolayer, where the twisting is the greatest and there are fewer interactions per rod, is not more energetically advantaged or disadvantaged by the twisting than the rest of the cluster.

At higher temperature [$T = 0.16$, Fig. S7 (c)], the driving forces change, with the rod entropy now driving the twist at all angles and the potential energy always opposing the twist. This indicates that twisting becomes increasingly driven by the rod entropy as the monolayer density decreases. Consistent with this, we observe a similar change for depletion-driven twisting as the polymer fugacity decreases, i.e. with the rod entropy F_r increasingly favoring twisting at small twists (e.g., $\mu_p = 0.8$) in the depletion-driven case of straight rods [see Fig. S8 compared to Fig.3a in the main text].

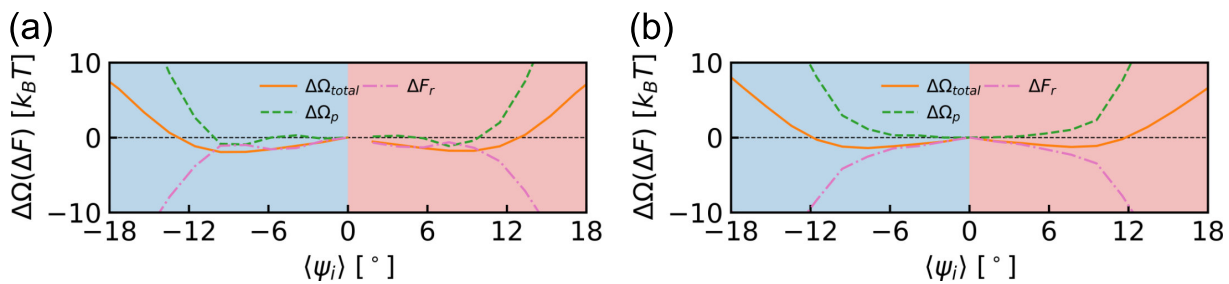


FIG. S8. The change in total free energy ($\Delta\Omega_{total}$) and its decomposition (ΔF_r and $\Delta\Omega_p$) as a function of the twist ($\langle\psi_i\rangle$) for a monolayer formed by $N_r = 37$ straight rods at a polymer fugacity of (a) $z_p = 1.0$ and (b) $z_p = 0.8$.

-
- [S1] J. A. Wood, Y. Liu, and A. Widmer-Cooper, *J. Chem. Phys.* **154**, 244505 (2021).
[S2] E. J. Meijer and D. Frenkel, *J. Chem. Phys.* **100**, 6873 (1994).
[S3] M. R. Shirts and J. D. Chodera, *J. Chem. Phys.* **129**, 124105 (2008), 0801.1426.
[S4] L. Kang, T. Gibaud, Z. Dogic, and T. C. Lubensky, *Soft Matter* **12**, 386 (2016).